



This is a repository copy of *Localized damage analysis for high strength S960 steel using micro-tensile testing and digital image correlation*.

White Rose Research Online URL for this paper:

<http://eprints.whiterose.ac.uk/152303/>

Version: Published Version

---

#### **Proceedings Paper:**

Dowding, R.G., Pinna, C. orcid.org/0000-0002-9079-1381, Ghadbeigi, H. orcid.org/0000-0001-6507-2353 et al. (1 more author) (2018) Localized damage analysis for high strength S960 steel using micro-tensile testing and digital image correlation. In: Ubiquity Proceedings. 5th International Small Sample Test Techniques Conference, 10-12 Jul 2018, Swansea, Wales. Ubiquity Press, Ltd. , p. 16.

<https://doi.org/10.5334/uproc.16>

---

#### **Reuse**

This article is distributed under the terms of the Creative Commons Attribution (CC BY) licence. This licence allows you to distribute, remix, tweak, and build upon the work, even commercially, as long as you credit the authors for the original work. More information and the full terms of the licence here:  
<https://creativecommons.org/licenses/>

#### **Takedown**

If you consider content in White Rose Research Online to be in breach of UK law, please notify us by emailing [eprints@whiterose.ac.uk](mailto:eprints@whiterose.ac.uk) including the URL of the record and the reason for the withdrawal request.



**Associated conference:** 5th International Small Sample Test Techniques Conference

**Conference location:** Swansea University, Bay Campus

**Conference date:** 10th - 12 July 2018

---

**How to cite:** Dowding, R.G. Pinna, C., Ghadbeigi, H., & Farrugia, D., 2018. Localized damage analysis for high strength S960 steel using micro-tensile testing and digital image correlation. *Ubiquity Proceedings*, 1(S1): 16 DOI: <https://doi.org/10.5334/uproc.16>

**Published on:** 10 September 2018

---

**Copyright:** © 2018 The Author(s). This is an open-access article distributed under the terms of the Creative Commons Attribution 4.0 International License (CC-BY 4.0), which permits unrestricted use, distribution, and reproduction in any medium, provided the original author and source are credited. See <http://creativecommons.org/licenses/by/4.0/>.

## UBIQUITY PROCEEDINGS

Ju [ ubiquity press ] <https://ubiquityproceedings.com>

# Localized damage analysis for high strength S960 steel using micro-tensile testing and digital image correlation

R.G. Dowding <sup>1\*</sup>, C. Pinna <sup>2</sup>, H. Ghadbeigi <sup>3</sup> and D. Farrugia <sup>4</sup>

<sup>1</sup> The University of Sheffield; rdowding1@sheffield.ac.uk

<sup>2</sup> The University of Sheffield; c.pinna@sheffield.ac.uk

<sup>3</sup> The University of Sheffield; h.ghadbeigi@sheffield.ac.uk

<sup>4</sup> Tata Steel UK Limited didier.farrugia@tatasteel.com

\* Correspondence: rdowding1@sheffield.ac.uk

**Abstract:** In-situ interrupted tensile tests combined with Digital Image Correlation (DIC) were performed on S960 hot rolled steel to identify damage initiation on the surface of the sample. Shear bands and damage initiation and evolution in the microstructure were observed during the test. It was found that shear bands are generated on the surface as plastic deformation occurs. Void nucleation was found to be initiated where a large plastic deformation gradient is observed.

**Keywords:** Steel; DIC; Damage; Microscale tensile

## 1. Introduction

High strength steels used in structural elements have a reduced bendability compared to lower strength steels, limiting manufacturing processes. Previous work has found shear bands to be prevalent on the outer, tensile stressed region of the bend [1]. This localization of strain is the source of failure in bending [2].

Work has been undertaken to identify the failure mechanism for 3 point bending in high strength S960 steel. To better understand damage initiation in bending, tensile tests have been performed inside a Scanning Electron Microscope (SEM) to identify failure mechanisms in the sample. These failure mechanisms can then be compared to those observed in bending tests.

Similar work has been used to determine the strain bands, localized strains in microstructures and damage initiation mechanism in Dual Phase (DP) steels, consisting of martensitic and ferritic phases [3], however the micro mechanisms of deformation and damage in S700, S960 and S1100 have not been studied before.

## 2. Materials and Methods

The material is an experimental lab produced hot rolled S960 grade steel with a thickness of 6mm that contains martensitic and bainitic microstructures. The sample geometry as developed by Ghadbeigi et. al. [3] was used in this study in order to ensure the deformation is localized within the field of view of the microscope at high magnifications. Fig. 1 shows the selected geometry and associated dimensions of the samples used.

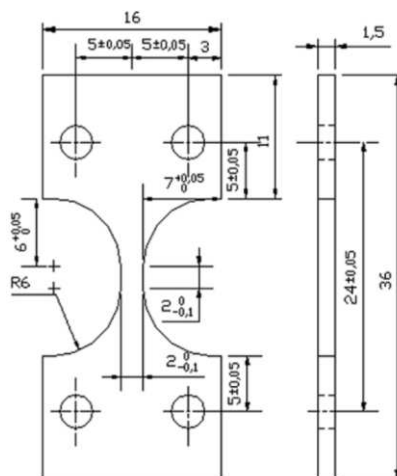


**Figure 1.** Tensile test sample dimensions for use within the SEM [3].

This sample was then ground and polished to remove material with residual stresses, deformations from machining and obtain a polished surface. Chemical etching using 2% nital solution was then used to reveal the microstructure of the steel. Lines were engraved onto the sample as shown in Fig. 2, to evaluate elongation of the gauge length optically. The tensile test was then carried out with regular interruptions to record images of the area of interest in the gauge length of the microstructure up to fracture of the specimen. The etched microstructure provides identifiable patterns that can be processed by the Davis DIC software [4] to produce strain maps as used by Al-Harbi et al [5].

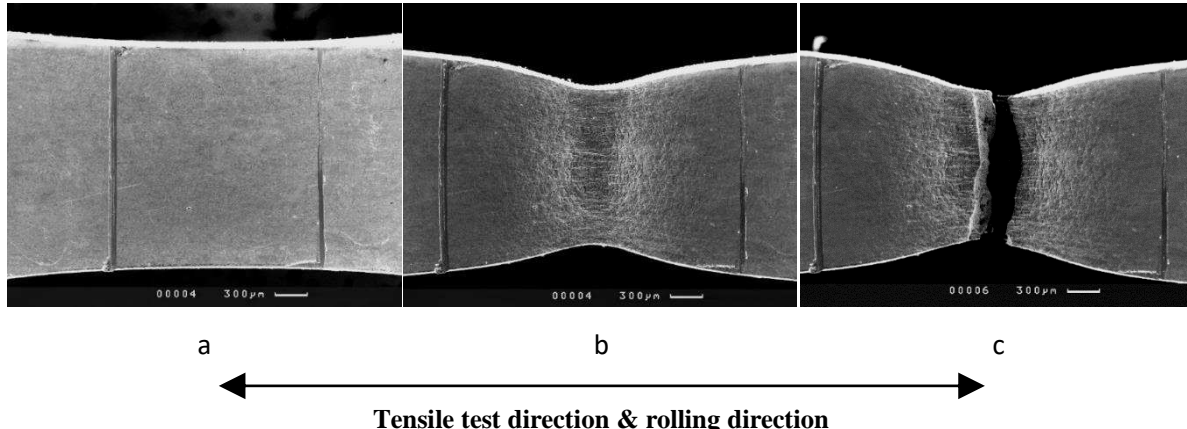


**Figure 2.** Images of the gauge length at 30x magnification during a tensile test. **a)** No deformation **b)** necking at 57% plastic strain and **c)** failure.

### 3. Results

Using these methods we can produce stress strain curves from the tensile test and identify void nucleation points and their localized strain using DIC. These are analyzed to understand the formation of damage leading to failure of the sample.

#### 3.1. Plastic deformation curve

By performing a tensile test a stress strain curve was obtained. Since only the plastic region is of interest, the stress-plastic strain curve was created free of elastic effects as shown in Fig. 3.

The steel reaches its elastic limit at 976MPa and UTS at 1102MPa, maximum elongation reaches 58%. The elongation is exaggerated by the sample geometry and is reported to be of an order of 5 times greater than a standard tensile test [3]. This is due to the sample geometry extending the post uniform section of the stress strain curve due to the stress triaxiality state being different to a standard tensile test specimen. This extends the testing of the sample providing better conditions to study damage development in the microstructure.

#### 3.2. SEM micrographs

Low magnification micrographs of the specimen are shown in Fig. 2. It can be seen that the sample undergoes a significant amount of necking and elongation in image Fig. 3b) with the surface becoming rough, therefore highlighting the very large plastic deformation experienced by the microstructure.

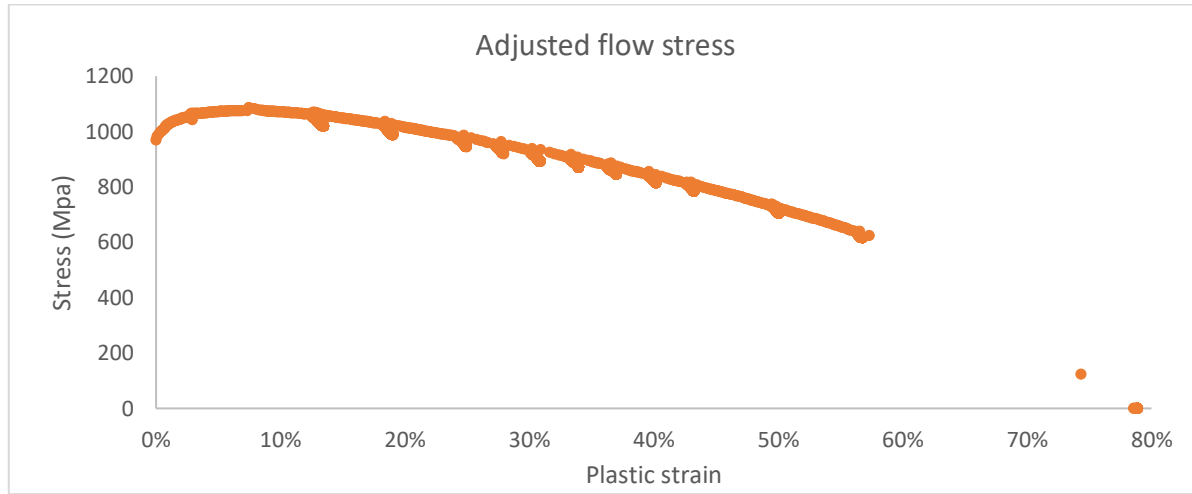


**Figure 3.** Stiffness adjusted stress vs strain curve for the tensile test parallel to the rolling direction for S960 steel.

### 3.3. Strain Maps

Micrographs from Fig. 4 were processed in Deben 8.4.0. This was using the sum of differences correlation mode, with a step size of 15 and subset of 35 pixels. The mapping is displaying strain parallel to the tensile test direction.

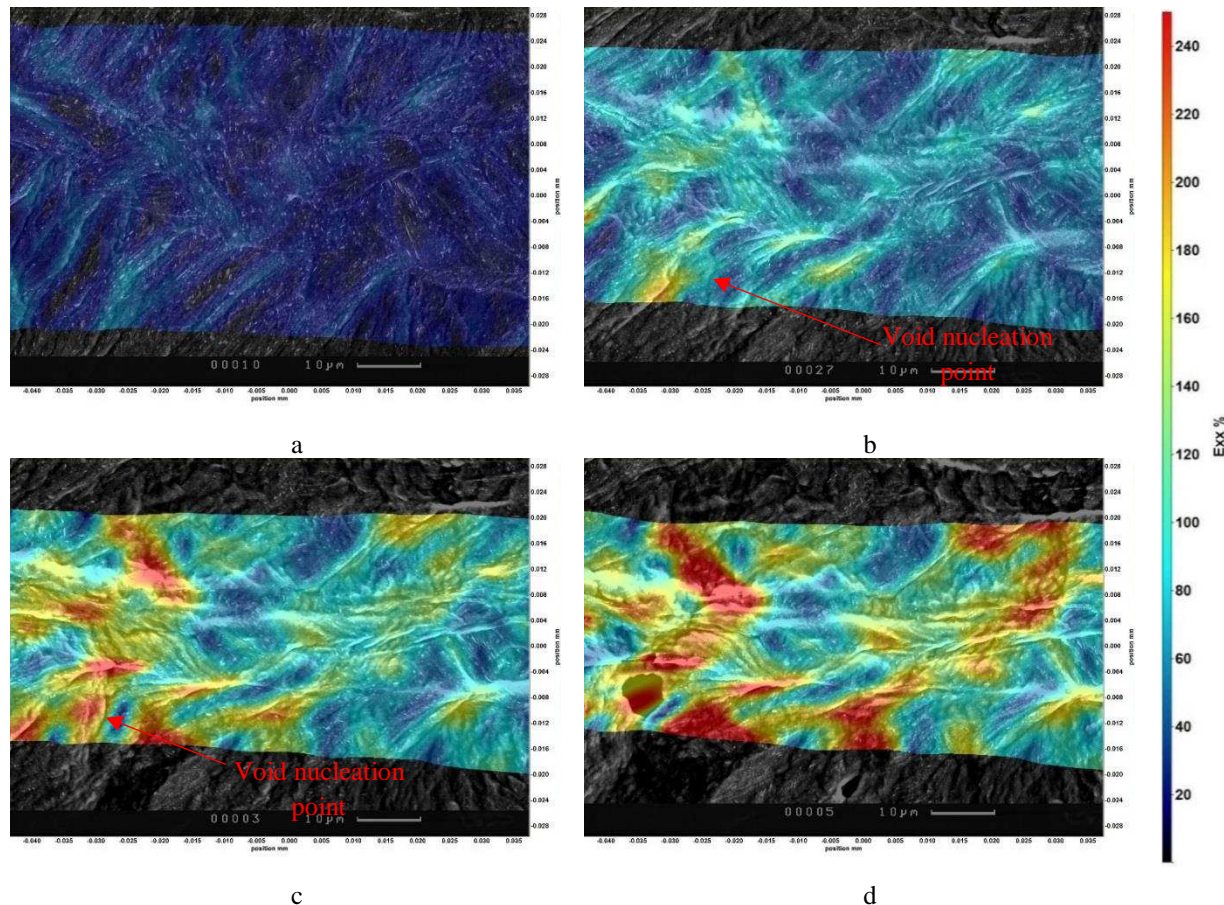


**Figure 4.** Tensile strain maps overlaid on the microstructure images produced using high magnification SEM images processed using Davis [4], **a)** 19% plastic strain **b)** 40% plastic strain, **c)** 50% plastic strain **d)** last image prior to failure, 57% plastic strain.

Once plastic deformation occurs within the sample, shear bands become visible at around 45 degrees to the tensile test direction in Fig4a) and b). Strain localizes in these bands which become very clearly defined by the end of the test due to the high strain gradient with the surrounding regions of the microstructure. As shown in Fig4 b) and c) the void nucleation point is found in a region straddling a shear band and a low strain point. It is found that the void is generated at 160% strain with the high strain region reaching values up to 240% and a lowest point of 8% strain. Due to the triaxiality of the sample, the failure begins at the center of the sample and the images are of the failure reaching the surface. The maximum and minimum strain values are found to be 5 $\mu$ m apart from one another. This high strain differential is enough to cause a failure that cracks proceed off leading to failure shortly after Fig4d) was acquired.

There is a second crack that formed off another void at the bottom of Fig4d). This crack follows another shear band showing the importance of shear bands in this steel's failure. These voids are nucleating from the subsurface and more instances of the damage are required to better understand how this steel fails. In bending, the failure occurs due to shear bands and this work highlights that the tensile test failure is also affected by shear bands. The procedure also shows that strain mapping can be obtained with good correlation even with high strains when imaging S960 high strength steels.

As shown in Fig. 5, a series of images are acquired until the sample failed from a-d. It can be seen how the surface becomes visibly rough through the tensile test. Eventually bright lines running parallel to the tensile test direction become prevalent as out of plane deformation occurs. Finally cracks and voids nucleate at the surface in image d. All images were then processed by DIC to produce stain maps for the analysis of damage development in relation to strain distributions. This presented difficulties for the operator, particularly maintaining the images in the same position, in focus and adjusting the brightness and contrast as beam contamination and out of plane deformation occurred on the sample. Doing this results in better correlation with DIC. Even with this deformation using Davis DIC software with sum of differential correlation mode a satisfactory strain map can be produced.

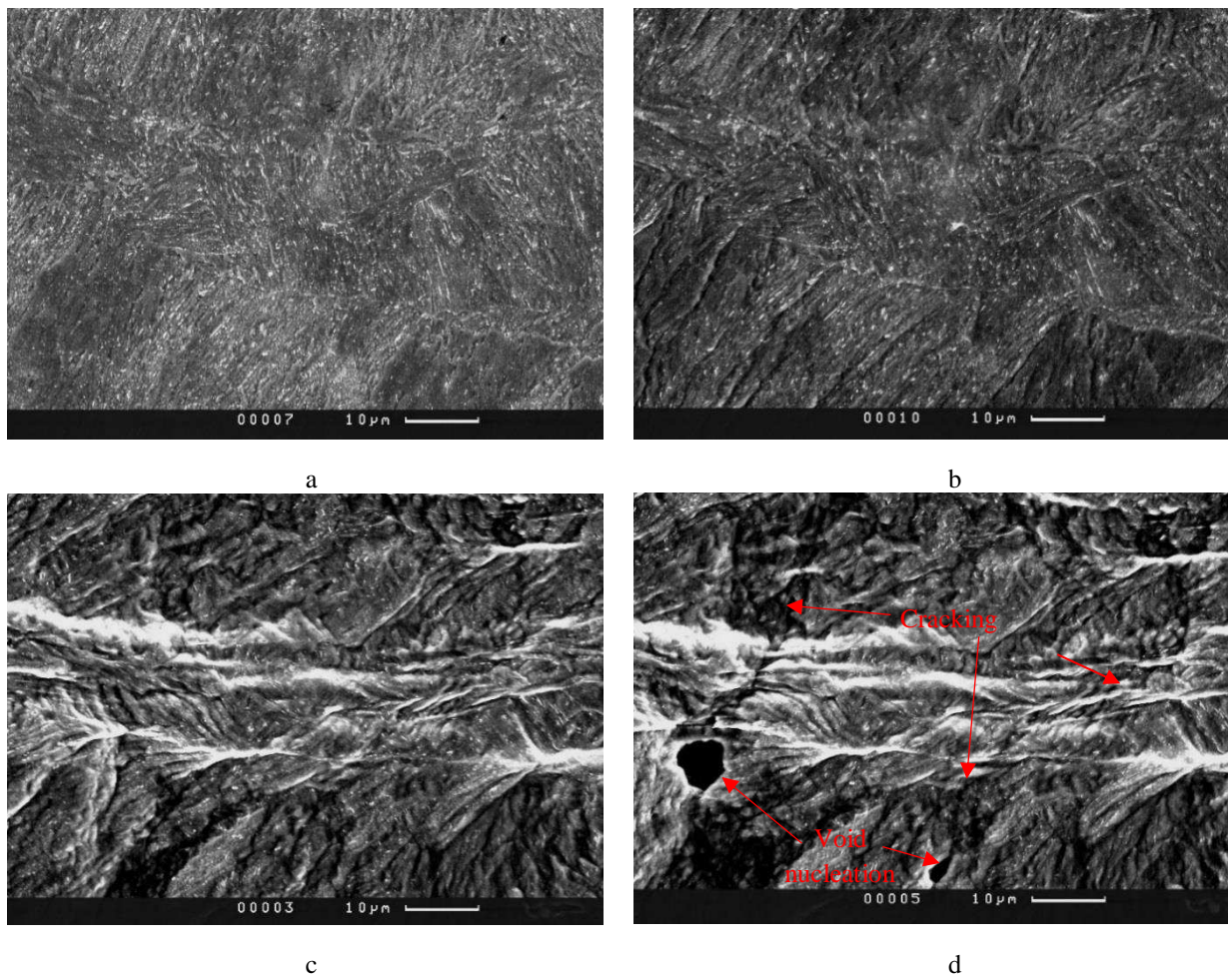


**Figure 5.** High magnification SEM images at 1400x of the tensile test sample, **a)** No deformation **b)** 19% plastic strain **c)** 50% plastic strain **d)** last image prior to failure; 57% plastic strain.

#### **4. Conclusions**

This work has demonstrated that the combination of small-scale tensile testing and DIC can be successfully applied to the study of damage formation in S960 steels in relation to large strain distributions up to failure. Tensile strain values up to 240% have been recorded in the microstructure with damage nucleating at local values of 160%. Results have shown that damage forms at the boundary between high-strain shear bands and low-strain regions.

**Acknowledgments:** The authors would like to thank Tata Steel UK Limited and the EPSRC (iCase, Project Reference No: 180395) for funding this work.

#### **References**

1. Crowther, D.N.; Wen, S.; Wade, B.A. Shear band formation during bend testing of S960., Internal TATA steel presentation, 2015.
2. Kaijalainen, A.J.; Suikkanen, P.P.; Karjalainen, L.P.; Porter D.A. Influence of subsurface microstructure on the bendability of ultrahigh-strength strip steel. Materials Science & Engineering A, **2016**, 654, 151-160.
3. Ghadbeigi, H.; Pinna, P.; Celotto, S.; Yates, J. R. Local plastic strain evolution in a high strength dual phase steel, Materials Science & Engineering A, **2010**, 527, 5026-5032.
4. DaVis 8.4.0, LaVision GmbH.
5. Alharbi, K.; Ghadbeigi, H.; Efthymiadis, P.; Zanganeh, M.; Celotto, S.; Dashwood, R.; Pinna, C. Damage in dual phase steel DP1000 investigated using digital image correlation and microstructure simulation, Modelling Simul. Mater. Sci. Eng., **2015**, 23, 1-17.